Proton-Induced Crosslinking of CR 6-2 Polycarbonate

S. A. Nouh,[1] Amal Mohamed,[2] H. K. Marie[3]

[1]*Physics Department, Faculty of Science, Ain Shams University, Cairo, Egypt*
[2]*Physics Department, Faculty of science, Zagazig University, Cairo, Egypt*
[3]*Physics Department, Faculty of Science, Fayoum University, Cairo, Egypt*

Received 30 March 2008; accepted 18 December 2008
DOI 10.1002/app.29902
Published online 23 February 2009 in Wiley InterScience (www.interscience.wiley.com).

ABSTRACT: CR 6-2 polycarbonate samples were irradiated using different fluences (10^{11}–10^{14} ions/cm^2) of 1 MeV protons. The structural modifications in the proton-irradiated CR 6-2 samples have been studied as a function of fluence using different characterization techniques such as X-ray diffraction, intrinsic viscosity of the liquid samples, as a measure of the mean molecular mass, Fourier transform infrared spectroscopy, thermogravimetric analysis, differential thermal analysis, refractive index, color difference, and mechanical properties. The results indicate that the irradiation of CR 6-2 detector at the fluence range 1×10^{12}–5×10^{14} ions/cm^2 causes intermolecular crosslinking and allows the formation of covalent bonds between different chains, leading to a more compact structure of CR 6-2 polymer, which resulted in an improvement in its thermal, optical, and mechanical properties. Also, this crosslinking reduces the ordering structure and increases the amorphous regions that enhance the polymer resilience. © 2009 Wiley Periodicals, Inc. J Appl Polym Sci 112: 2724–2731, 2009

Key words: protons irradiation; polycarbonate; structural properties; thermal properties; mechanical properties

INTRODUCTION

Irradiation of polymers has established itself as one of the most acceptable approach to alter polymer properties significantly.[1–12] It destroys[13] the initial structure by cross linking, free radical formation, irreversible bond cleavages, etc., which results in the fragmentation of molecules and formation of saturated and unsaturated groups.[11] All these processes introduce the so-called defects inside the material that are responsible[2] for change in the optical, electrical, mechanical, and chemical properties of the material.

In this article, we have studied the structural modifications in the proton-irradiated CR 6-2 samples. Similar studies have been carried out by several other authors,[14–17] however in a different context. Tripathy et al.[14] have reported the decrease in transmittance of polyallyal diglycol carbonate (PADC) with the increase in proton fluence. Also, the thermal stability of PADC was found to be an inverse function of fluence. Lounis et al.[15] studied the characterization of chemical and optical modifications induced in CR-39 detectors by 22.5 MeV proton beams with fluences ranging from 10^{11} to 10^{14} particles/cm^2. Nilam et al.[16] have indicated that the hardness of the Kapton film increases significantly as the proton fluence increases. Also, there is an exponential increase in the conductivity with frequency but the effect of irradiation is not significant. Singh et al.[17] studied the thermal behavior of 3 MeV proton-irradiated polymeric blends of polyvinyl chloride and polyethylene terephthalate. Mishra et al.[18] determined the activation energy of thermal decomposition of proton-irradiated polymers. The ion irradiation of polymeric solids induces numerous modifications in the polymer properties, thus increasing their applicability in various fields.

From literature survey, it is noticed that the effects of protons irradiation on the physical properties of CR 6-2 polycarbonate have received less attention. This study deals with the investigation of the effect of proton irradiation on the structural, thermal, and mechanical properties of CR 6-2 polycarbonate not only to obtain information concerning the interaction of protons with CR 6-2 polycarbonate but also to study the feasibility of enhancing its properties, improving its performance in different fields.

EXPERIMENTAL

Samples

CR 6-2 is a polycarbonate with a chemical composition of $C_{16}H_{14}O_3$ blended with polyester (PC/PBT blend film). It is manufactured by Bayer A. G.

Correspondence to: S. A. Nouh (samirnouh90@hotmail.com).

(Leverkusen, Germany), with an average thickness of 250 μm and density 1.23 g/cm^3.

Irradiation facilities

The CR 6-2 samples have been exposed to perpendicular 1 MeV proton beams of different fluences in the range 10^{11} – 10^{14} ions/cm^2, with the sample held at a vacuum of 10^{-6} Torr. The current density of the proton beam was 0.05 μA/cm^2 and the beam diameter was 0.2 mm.

Analysis of irradiated samples

The X-ray diffraction measurements were carried out with a Philips powder diffractometer type PW 1373 goniometer. The diffractometer was equipped with a graphite monochromator crystal. The wavelength of the X-rays was 1.5405 Å, and the diffraction patterns were recorded in the 2θ range (4°–40°) with scanning speed of 2°/min.

The viscosity measurements were carried out in Oswald viscometer of the type pinkevitch size 0 No. 2106, manufactured by Poulten, Self, and Lee, Ltd. (Wickford, Essex, England). This viscometer was calibrated in accordance with the standard method of test for kinematic viscosity specified in ASTM D-445-IP 71. The viscosity measurements were carried out at 35, 40, 45, and 50°C using a bridge-controlled thermostat bath E-270 Series III, manufactured by Pownson of Mercer Ltd., Croydon Edinburgh, Oxford.

Fourier transform infrared spectra (FTIR) were recorded using model Shimadzu 8201 PC. All the measurements were done in the range of 4000 to 400 cm^{-1}. The spectra were obtained for the absorbance of the polymer as a function of wavenumber with resolution 1 cm^{-1} and accuracy better than ±4 cm^{-1}.

The thermal behavior was investigated using differential thermal analysis (DTA) and thermogravimetric analysis (TGA) with a differential scanning calorimeter (DSC) Setaram Labsys TG–DSC16 instrument. α-Al_2O_3 powder was used as a reference for the DTA measurements. Thermal experiments were carried out on all samples at a heating rate of 10°C/min with Ar as carrier gas at a flow rate of 30 cm^3/min.

The refractive index measurements were carried out using an Abbe refractometer (Type Reichert; mark II, Model-10480, New York). The accuracy of measuring the values of refractive indices, surface temperature of the prism, and the wavelength of the light used were ±0.0001, 18.3–20.5°C, and 5893 Å, respectively. Several values were measured to the same sample and the average value were considered.

The transmission measurements were carried out at room temperature using a Shimadzu UV–Vis–NIR scanning spectrophotometer, type 3101 PC. This unit measures in the wavelength range from 200 to 3200 nm, with wavelength accuracy better than ±3 nm over 200–2000 nm and better than ±9 nm over 2000–3000.

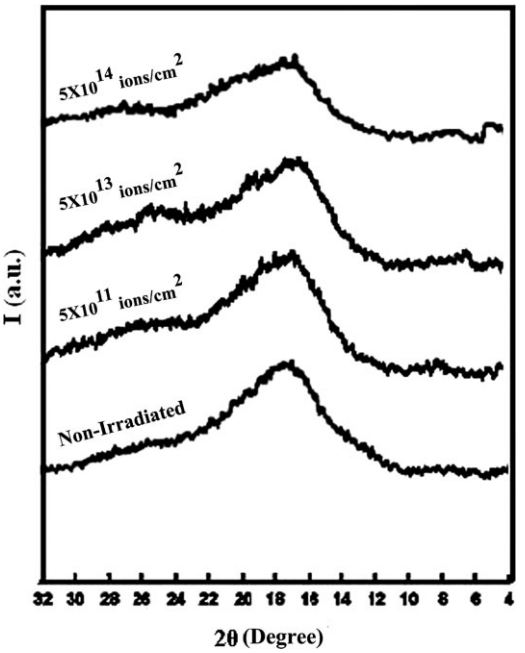

Figure 1 X-ray diffraction patterns of the nonirradiated and some irradiated CR 6-2 samples.

Mechanical measurements were carried out using Testometric M350–5Ax with 5-kN load cell at room temperature. Dumbbell–shaped samples of standard dimensions (50-mm long with a neck of 27 mm and width of 3 mm) were placed between the jaws, and the load was applied at a rate of 50 mm/min until failure occurred. Five pieces of the same sample were used, and results were averaged for each data point.

RESULTS AND DISCUSSION

The projected range of 1 MeV proton beams in CR 6-2 was calculated to be 100 μm using SRIM 2000 code, Ziegler et al.,[18] which is smaller than the thickness of the CR 6-2 sample. Then, all the 1 MeV energy is deposited inside the sample.

Structural properties

X-ray diffraction

The CR 6-2 polymer is not entirely crystalline. The chains or parts of chains, which are not in the crystals, have no order to the arrangement. So, the CR 6-2 polymer really has two components, the crystalline portion and amorphous portion. The X-ray

TABLE I
Values of Integral Intensity (*I*) and Full Width at Half Maximal Intensity (Δ*W*) as a Function of Proton Fluence

Proton fluence (ions/cm^2)	*I* (a.u.)	Δ*W* (Radian)
0.00	13.8	6.5
1.00E + 11	16.4	6.2
5.00E11	18.8	6.0
1.00E + 12	19.4	5.5
5.00E + 12	14.3	5.6
1.00E + 13	12.8	6.6
5.00E + 13	10.1	7
1.00E + 14	9.4	7.3
5.00E + 14	8.7	7.5

diffraction patterns of the nonirradiated and irradiated CR 6-2 samples were recorded. Figure 1 shows the diffraction patterns for the nonirradiated and some irradiated samples. It is found that these patterns were characterized by halos extending in the 2θ range 10°–26° with maximum diffraction intensity (peak) has been observed at 2θ = 18°. The profile of the halos shows that the CR 6-2 polymer is an amorphous polymer with some ordering within the amorphous phase. The area under these halos is proportional to the integral scattering intensity of the X-rays. The integral intensity of the halos was calculated; approximate indicative values are given in Table I as a function of the proton fluence. The values indicate that the integral intensity increases up to a maximum value around the 1×10^{12} ions/cm^2 irradiated sample, and then decreases with increasing the proton fluence up to 5×10^{14} ions/cm^2.

Since the halo's width at the half of maximal intensity Δ*W* can give information about the amount of ordering within the amorphous regions, approximate indicative values of Δ*W* were calculated and are given in Table I. The results indicated that the half-width shows an opposite trend to that of the integral intensity, where it decreases until a minimum value around the 1×10^{12} ions/cm^2 irradiated sample, and then increases with increasing the fluence up to 5×10^{14} ions/cm^2.

The increase in integral intensity indicates an increase in the ordering character of the polymer samples, which can be attributed to degradation (chain scission) induced by proton irradiation. This scission can reduce the number of entanglements per molecule. Chain scission can also act to relieve intermolecular stress in the amorphous region, thus increasing chain mobility. The increase in mobility permits some molecules to reordered.[19]

On the other hand, the decrease in integral intensity in the fluence range 1×10^{12}–5×10^{14} ions/cm^2 denotes a decrease in the ordering in the samples, indicating that the ordering structure has been destroyed. This could be attributed to the crosslinking that changes the previously regularly arranged portions into nonarranged ones by forming new bonds between chains. This means that crosslinking is the predominant effect in this fluence range.

Intrinsic viscosity

Solutions of different concentrations (0.2, 0.4, 0.6, and 0.8%) were prepared from the nonirradiated and irradiated CR 6-2 sheets using pure chloroform as a solvent. These diluted solutions were chosen to avoid any attractive secondary interactions between the polymer and solvent molecules, which can be reflected in an increase of the viscosity in ways that accurate measurements cannot be made. The kinematic viscosity of the liquid samples can be calculated by the product of the observed time of flow and the capillary constant of the viscometer. The result is always expressed as relative viscosity (η_{rel}), calculated as the ratio of the viscosities of polymer solution and the pure solvent. Additional values may be calculated such as specific viscosity ($\eta_{spc} = \eta_{rel} - 1$), a reduced viscosity ($\eta_{red} = \eta_{spc}$/concentration), and intrinsic viscosity, the limiting viscosity number (η_{in}= lim η_{red} when the concentration tends to zero) that is related to the mean molecular mass of the dissolved polymer and can give a qualitative idea of whether molecular weight is high or low.

The intrinsic viscosity of the CR 6-2 solutions was measured at different temperatures (35, 40, 45, and 50°C). Figure 2 shows the variation of the intrinsic viscosity and the proton fluence. The figure shows that the intrinsic viscosity decreases until a minimum value around the 1×10^{12} ions/cm^2 irradiated sample and then increases on increasing the proton fluence up to 5×10^{14} ions/cm^2. The fluence range

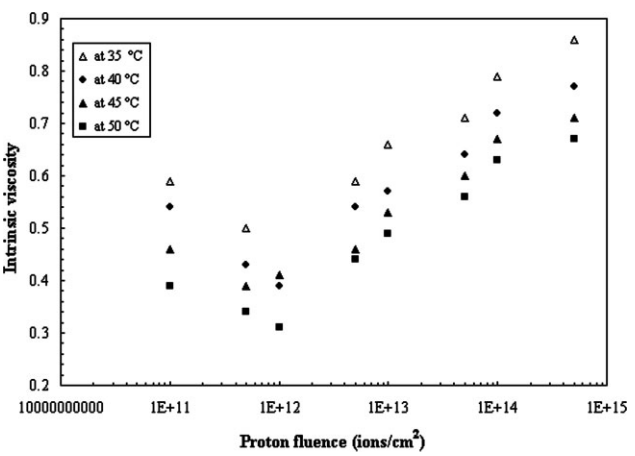

Figure 2 Variation of intrinsic viscosity, measured at different temperatures, for the CR 6-2 liquid samples, with the proton fluence.

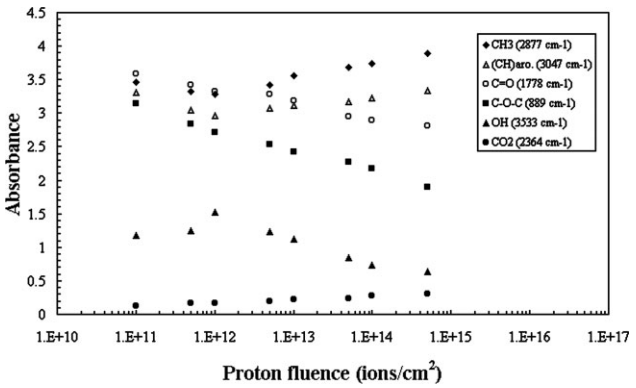

Figure 3 Variation of absorbance, measured at the characteristic wavenumbers, with the proton fluence.

in which the intrinsic viscosity decreases can be explained by the formation of shorter molecules as a result of degradation, which causes both a random breaking of bonds and the formation of stable molecules with a lower molecular weight.[20] While the increases in intrinsic viscosity in the fluence range from 1×10^{12} to 5×10^{14} ions/cm^2 indicates an increase in the molecular mass of the polymer due to crosslinking process.

The effect of temperature on the intrinsic viscosity of CR 6-2 polymer was investigated. The results indicated that the intrinsic viscosity decreases with temperature. This can be attributed to the temperature that causes a simple thermal activation.

Fourier transform infrared

The FTIR spectral analysis has been performed to investigate the structural changes induced in the CR 6-2 polymer due to proton irradiation. The changes have been estimated from the relative increase or decrease in the intensity of the peak associated to the functional groups present in the polymer.

The material used in this study is aromatic polycarbonate. Its functional groups include methyl, phenyl ring, carbonyl, ether, and hydroxyl. The absorbance of different bands coming from the same functional group exhibits the same trend with the proton fluence. So, each characteristic group of polycarbonate is represented by only one wavenumber. Values of the absorbance of these bands were calculated and plotted in Figure 3 as a function of the proton fluence. From the figure it is clear that the absorbance measured at the wavenumbers 1778 and 889 cm^{-1} decreases with the increasing proton fluence up to 5×10^{14} ions/cm^2, indicating the breaking of the C=O and C—O—C bonds.

The absorbance measured at the wavenumber 2877 and 3047 cm^{-1} shows a decrease in the intensity of C—H bond until a minimum value around the 1×10^{12} ions/cm^2 irradiated sample, followed by an increase on increasing the proton fluence up to 5×10^{14} ions/cm^2.

The intensity of the peak corresponding to OH group (3533 cm^{-1}) increases at the proton fluence range $1 \times 10^{12} - 5 \times 10^{14}$ ions/cm^2. These results indicate that scission takes place at the carbonate site with the probable elimination of carbon dioxide/carbon monoxide and the formation of hydroxyl group. The abstraction of —H may be from isopropyl or aromatic group.[21] The increase in the hydroxyl groups in the fluence range up to 1×10^{12} ions/cm^2, which means an increase in the end groups of macromolecules, indicates that degradation process prevails in this fluence range. Above 1×10^{12} and up to 5×10^{14} ions/cm^2, an opposite trend has been observed because of the formation of bonds through crosslinking mechanism.

Thermal analysis techniques

Thermogravimetric analysis

Thermogravimetric analysis (TGA) was performed on CR 6-2 samples to get a better understanding of the changes in its thermal stability due to the proton irradiation. TGA was performed for nonirradiated and irradiated samples in the temperature range from room temperature to 600°C, at a heating rate of 10°C/min. The results indicated that the CR 6-2 samples decompose in one main weight-loss stage.

Using the TGA thermograms, the values of onset temperature of decomposition T_0, the temperature at which the decomposition starts, were calculated. Figure 4 shows the variation of T_0 with the proton fluence. From the figure it is clear that T_0 decreases until a minimum value around the 1×10^{12} ions/cm^2 irradiated sample followed by an increase on increasing the proton fluence up to 5×10^{14} ions/cm^2.

These results support that the degradation is the dominant phenomenon in the fluence range up to 1×10^{12} ions/cm^2. Degradation led to the formation of low-molecular-weight products, which decrease the strength of the polymer, thereby decreasing its ability to withstand high temperatures.[22] At the fluence range 1×10^{12}–5×10^{14} ions/cm^2, the opposite effect was observed indicating that the samples regain their thermal stabilities due to crosslinking process, which gives strength to the polymer against thermal degradation.[23]

Activation energy of thermal decomposition (E_a)

Various thermogravimetric mathematical methods based on either the rate of conversion or the heating rate have been reported to determine the kinetic parameters of thermal degradation. The method

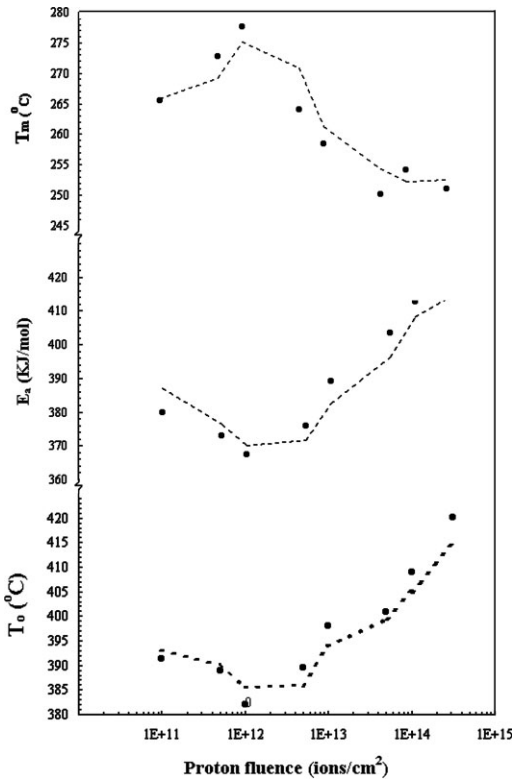

Figure 4 Variation of the onset temperature of decomposition T_0, activation energy of thermal decomposition E_a, and melting temperature T_m with the proton fluence.

proposed by Horowitz and Metzger[24] has been used in this study for the measurements of the thermal activation energies.

Using the TGA data, values of activation energy of thermal decomposition E_a were calculated. Figure 4 shows the variation of E_a with the proton fluence. The figure shows that E_a exhibited a similar trend to that of T_0, where it decreases until a minimum value around the 1×10^{12} ions/cm^2 irradiated sample, indicating an increase in the thermal degradation rate. Above 1×10^{12} and up to 5×10^{14} ions/cm^2, it increases leading to an increase in the thermal decomposition rate.

At the fluence range 0–1×10^{12} ions/cm^2, the proton irradiation leads to an acceleration of thermal degradation; this can be attributed to the change in structure, which causes the thermal degradation to go through another pathway with higher rate of degradation. The opposite effect was observed in the fluence range 1×10^{12}–5×10^{14} ions/cm^2. This may be due to the re-formation of the initial structure in the polymer.

Differential thermal analysis

Differential thermal analysis (DTA) was performed in the temperature range from room temperature to 500°C, at a heating rate of 10°C/min on the non irradiated and irradiated CR 6-2 samples. All the thermograms were characterized by the appearance of one endothermic peak at the melting temperature.

Values of these melting temperatures are plotted as a function of the proton fluence in Figure 4. The figure shows that the melting temperature T_m exhibited an opposite trend to that of T_0 and E_a. It shows an increase up to a maximum value around the 1×10^{12} ions/cm^2 irradiated sample followed by a decrease with increasing the proton fluence up to 5×10^{14} ions/cm^2. The apparent discrepancy between the dependence of T_0 and T_m on fluence results from the fact that T_m is sensing the ordering structure of the polymer. It is possible to speculate that at low fluences 0–1×10^{12} ions/cm^2, the thickness of crystalline structures (lamellae) is increased, whereas at higher fluences 1×10^{12}–5×10^{14} ions/cm^2, the crosslinking destroys the ordering structure depressing the melting temperature.

Optical properties

Refractive index

The refractive indices of solid sheets of CR 6-2, exposed to proton irradiation up to 5×10^{14} ions/cm^2, were measured. The accuracy of measuring the values of refractive indices, surface temperature of the prism, and the wavelength of the light used were ±0.0001, 18.3–20.5°C, and 5893 Å, respectively. Figure 5 illustrates the variation of the refractive index with proton fluence. The refractive index showed a decrease in magnitude until a minimum value at around 1×10^{12} ions/cm^2 followed by an increase on increasing the fluence up to 5×10^{14} ions/cm^2. This behavior can be explained in terms of degradation and crosslinking induced by protons. Such behavior facilitates the formation of free radicals that are chemically active. This allows the

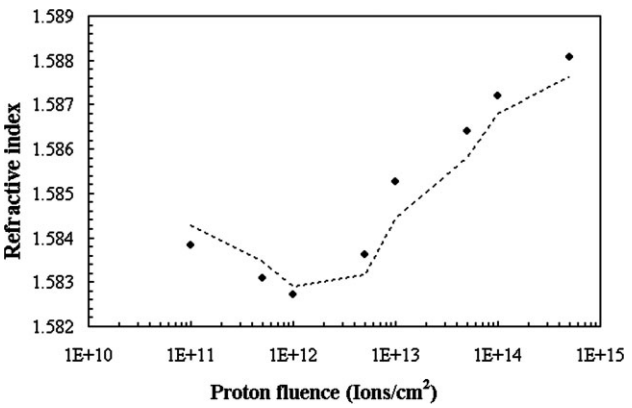

Figure 5 Variation of refractive index with the proton fluence.

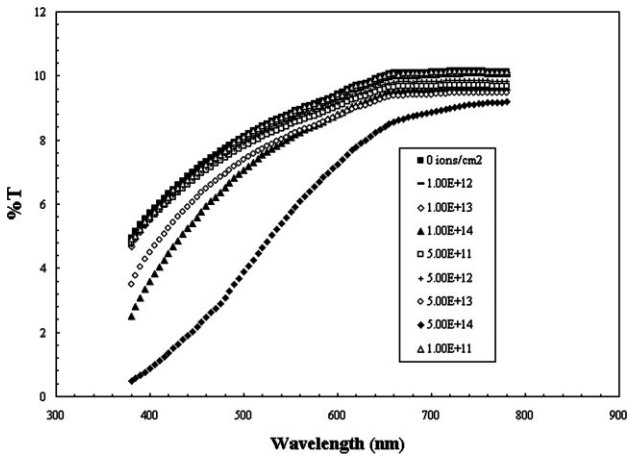

Figure 6 The transmittance of the CR 6-2 samples in the wavelength range 380–780 nm.

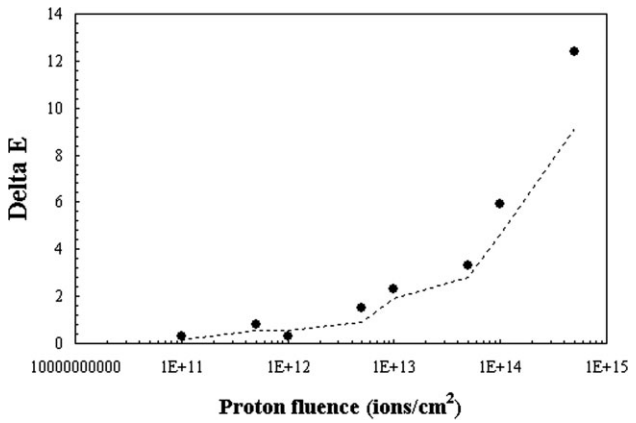

Figure 8 Variation of color intensity ΔE^* with the proton fluence.

formation of covalent bonds between different chains (crosslinking) and in turn minimizes the anisotropic character of the CR 6-2 polymer, leading to the increase in refractive index.[25] These results are in good agreement with those obtained by Shams-Eldin et al.[26] They illustrated that the incident radiations activate the main polymer chain implying a main-chain scission, which result in the decrease of the refractive index. The same effect was also investigated by Ranby and Rebek.[27]

Color changes

The transmission spectra measured in the wavelength range 200–3000 nm of the irradiated and nonirradiated CR 6-2 samples was measured. Figure 6 shows the transmittance of the samples in the wavelength range 380–780 nm.

The variation of the color intercepts L^*, a^*, and b^* with the proton fluence is shown in Figure 7. The accuracy in measuring L^* is ± 0.05 and ± 0.01 for a^* and b^*. It can be seen that the color parameters were significantly changed after exposure to proton irradiation. The green ($-a^*$) and blue ($-b^*$) color components of the nonirradiated film was changed to red ($+a^*$) and yellow ($+b^*$) after exposure to protons in the fluence range from 1×10^{12} to 5×10^{14} ions/cm^2. This is accompanied by an increase in the darkness of the samples ($-L^*$).

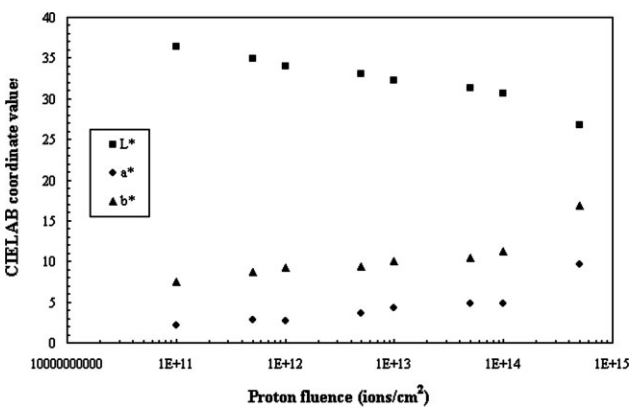

Figure 7 Variation of the color intercepts L^*, a^*, and b^* with the proton fluence.

The color intensity ΔE^*, which is the difference between the nonirradiated sample and those irradiated with different proton fluences was calculated and plotted in Figure 8 as a function of proton fluence. The color intensity ΔE^* was greatly increased with increasing the proton fluence and accompanied by a significant increase in the red and yellow color components ($+a^*$), ($+b^*$). This indicates that the CR 6-2 polymer has more response to color change by proton irradiation. These changes in color can be attributed to the trapping of the excited free radicals that are formed by ionization. Also, the trapped free radicals resulting from radiation-induced rupture of polymer molecules have electrons with unpaired spin. Such species may also give optical coloration.

Mechanical properties

A set of stress–strain curves for irradiated and nonirradiated CR 6-2 samples were measured. Those curves were obtained by continuously measuring the force developed as the sample is elongated at a constant rate of extension. Generally, the strain increases on increasing the stress due to the increase in the flexibility of the chain in the macromolecules.

The stress–strain curves serve to define several useful quantities including yield strength σ_y (the stress corresponding to a peak on the stress–strain

TABLE II
Values of the Yield Stress σ_y, Tensile Strength σ_f, Elongation at the Break ε_f, and the Young's Modulus E of CR 6-2 Samples as a Function of Proton Fluence

Proton fluence (ions/cm^2)	σ_y (MPa)	σ_f (MPa)	ε_f (%)	E (MPa)
0.00	62	47.2	121.5	2,460
1.00E + 11	56.2	44.32	123	2,320
5.00E11	54.1	42.4	126	2,290
1.00E + 12	52.5	40.5	129.3	2,260
5.00E + 12	59.8	43.6	118.4	2,380
1.00E + 13	64.2	47.8	114.4	2,410
5.00E + 13	65.6	49.7	110.2	2,520
1.00E + 14	67.8	53.5	107.2	2,580
5.00E + 14	68.5	56.4	106.9	2,640

curve), tensile strength σ_f (the stress corresponding to the fracture point), and fracture strain ε_f (elongation at the break).

The variation of σ_y, σ_f, and ε_f with the proton fluence is illustrated in Table II. It is clear that σ_y and σ_f exhibited the same trend with the proton fluence, as they decreased gradually with increasing the proton fluence up to 1×10^{12} ions/cm^2, and then increased with increasing the fluence up to 5×10^{14} ions/cm^2. The opposite trend could be observed for ε_f. The increase in yield stress may be attributed to the fact that high stresses enhance the flow mechanism by increasing the mobility of the macromolecular chains to yield higher flexibility. Also, at the fluence range 0–1×10^{12} ions/cm^2 in which σ_f decreases (while ε_f increases), the changes can be attributed to a degradation mechanism in which the standard chains and a great number of chain ends weaken and the material may become softer. On increasing the fluence above 1×10^{12} and up to 5×10^{14} ions/cm^2, crosslinking takes place.

Values of the Young's modulus E were calculated and are given in Table II. It is clear that the Young's modulus decreases until a minimum value around 1×10^{12} ions/cm^2. Above 1×10^{12} and up to 5×10^{14} ions/cm^2, it increases. The decrease in elastic modules indicates that the sample has become more flexible, which simply results from the decrease in interatomic force constants. Irradiation at proton fluence up to 1×10^{12} ions/cm^2 tend to allow the onset of rather localized rotational motions in many parts of the polymer molecules, and these motions are reflected in a decrease in the elastic modules.

CONCLUSION

The irradiation of CR 6-2 detector at the fluence range (1×10^{12}–5×10^{14} ions/cm^2) causes crosslinking, which reduces ordering and increases the amorphous regions that enhance polymer resilience.

The proton irradiation effects on the intrinsic viscosity of CR 6-2 polymer may be considered as a simple way to optimize its quality since the processing and application properties of that polymer depend very largely on its molecular structure.

The irradiation of CR 6-2 detector by protons in the fluence range (1×10^{12}–1×10^{14} ions/cm^2) led to further improvement in its thermal stability that enhances the scope of this polymer in high-temperature applications.

The proton irradiation at the fluence range 1×10^{12} – 5×10^{14} ions/cm^2 leads to an increase in refractive index due to crosslinking and thus minimizes the anisotropic character of the polymer.

The nonirradiated CR 6-2 polymer is nearly colorless; however, it showed significant color sensitivity toward proton irradiation.

The proton irradiation at the fluence range 0–1×10^{12} ions/cm^2 causes the standard chains and a great number of chain ends to be weaken and the material may become softer. Also, the decrease in elastic modules indicated that the sample has become more flexible, which simply results from the decrease in interatomic force constants.

References

1. Tanu, S.; Sanjeev, A.; Shyam, K.; Mittal, V.; Kalsi, P.; Manchanda, V. J Mater Sci 2007, 42, 1127.
2. Lee, E. Nucl Inst Methods Phys Res B 1999, 151, 29.
3. Schiestel, S.; Ensinger, W.; Wolf, G. Nucl Inst Methods Phys Res B 1994, 91, 473.
4. Phukan, T.; Kanjilal, D.; Goswami, T.; Das, H. Radiat Meas 2003, 36, 611.
5. Laskarakis, A.; Gravalidis, C.; Logothetidis, S. Nucl Inst Methods Phys Res B 2004, 216, 131.
6. Guenther, M.; Suchaneck, G.; Sahre, K.; Eichhorn, K.; Wolf, B.; Deineka, A.; Jastrabik, L. Surf Coat Technol 2002, 158, 108.
7. Taupiac, C.; Bennamane, B.; Decossas, J.; Vareille, J. Nucl Inst Methods Phys Res B 1997, 131, 198.
8. Mujahid, M.; Srivastava, D.; Gupta, S.; Avasthi, D. Radiat Phys Chem 2005, 74, 118.
9. Calcagno, L.; Compagnini, G.; Foti, G. Nucl Inst Methods Phys Res B 1992, 65, 413.
10. Steckenreiter, T.; Balanzat, E.; Fuess, H.; Trautmann, C. Nucl Inst Methods Phys Res B 1997, 131, 159.
11. Mokrani, Z.; Fromm, M.; Barillon, R.; Chambaudet, A.; Allab, M. Radiat Meas 2003, 36, 615.
12. Saad, A.; Awa, S.; Yokota, R.; Fujii, M. Radiat Meas 2005, 40, 780.
13. Marletta, G. Nucl Inst Methods Phys Res B 1990, 46, 295.
14. Tripathy, S.; Mishra, R.; Dwivedi, K.; Khathing, D.; Ghosh, S.; Fink, D. Radiat Meas 2001, 34, 15.
15. Lounis, Z.; Fromm, M.; Barillon, R.; Chambaudet, A.; Allab, X.; Radiat Meas 2003, 36, 615.
16. Nilam, S.; Singh, N.; Desai, C.; Singh, K. Radiat Meas 2003, 36, 699.
17. Singh, N.; Nilam, S.; Singh, K.; Desai, C. Radiat Meas 2005, 40, 741.

18. Mishra, R.; Tripathy, S.; Fink, D. Dwivedi, K. Radiat Meas; 2005 40, 754
19. Zhudi, Z.; Wenxue, Y.; Xinfang, C. Radiat Phys Chem 2002, 65, 173.
20. Nouh, S.; El-Mahdy, N.; Morsy, A.; Morsy, M. Radiat Meas 2005, 39, 471.
21. Nouh, S.; El-Tayeb, N.; Said, A.; Radwan, M.; El-Fiki, S. Radiat Meas 2007, 42, 8.
22. Mishra, R.; Tripathy, S.; Dwivedi, K.; Khathing, D.; Ghosh, S.; Muller, S.; Fink, D. Radiat Meas 2003, 37, 247.
23. Mishra, R.; Tripathy, S.; Dwivedi, K.; Ghosh, S.; Fink, D. Radiat Meas 2003, 36, 719.
24. Horowitz, H.; Metzger, G. Anal Chem 1963, 35, 1464.
25. Nouh, S. Radiat Meas 1997, 27, 499.
26. Shams-Eldin, M.; Wochnowski, C.; Koerdt, M.; Metev, S.; Hamza, A.; Juptner, W. Opt Mater 2005, 27, 1138.
27. Ranby, B.; Rebek, J. In Photodegradation, Photooxidation and Photostabilization of Polymers: Principles and Applications; Rabek, J. F., Ed. Wiley: 1996; p 153.